This version: 28.01.2023

Seaweed as a resilient food solution after a nuclear war

Florian Ulrich Jehn[1,2,*], Farrah Jasmine Dingal[1,3], Aron Mill[1], Cheryl Harrison[4], Ekaterina Ilin[5], Michael Y. Roleda[6], David Denkenberger[1,7]

[1] Alliance to Feed the Earth in Disasters, ALLFED, USA

[2] Justus-Liebig-University, Gießen, Germany

[3] Department of Energy and Mineral Engineering, The Pennsylvania State University, PA, USA

[4] Department of Ocean and Coastal Science, Center for Computation and Technology, Louisiana State University, Baton Rouge, LA, USA

[5] Leibniz Institute for Astrophysics Potsdam (AIP), Potsdam, Germany

[6] The Marine Science Institute, University of the Philippines Diliman, Quezon City, Philippines

[7] Department of Mechanical Engineering, University of Canterbury, Christchurch, Canterbury, New Zealand

*Corresponding author name(s).

Email: florian@allfed.info

Author Contributions: FUJ, AM, DD, CH were responsible for the design of this study. The data analysis was performed by FUJ, AM and EI. All authors contributed significantly to the interpretation of the data and the writing of the manuscript.

Competing Interest Statement: The authors declare that they have no known competing financial interests or personal relationships that could have influenced the following analysis.

Classification: Major: Agricultural Sciences; Minor: Sustainability Sciences

Keywords: Nuclear Winter, Seaweed, Abrupt Sunlight Reduction Scenario, Food Security, Nuclear War

This PDF file includes: Main Text, Figures 1 to 5, Figure S1-S16

Abstract

Abrupt sunlight reduction scenarios such as a nuclear winter caused by the burning of cities in a nuclear war, an asteroid/comet impact or an eruption of a large volcano inject large amounts of particles in the atmosphere, which limit sunlight. This would decimate agriculture as it is practiced today. We therefore need resilient food sources for such an event. One promising candidate is seaweed, as it can grow quickly in a wide range of environmental conditions. To explore the feasibility of seaweed after nuclear war, we simulate the growth of seaweed on a global scale using an empirical model based on *Gracilaria tikvahiae* forced by nuclear winter climate simulations. We assess how quickly global seaweed production could be scaled to provide a significant fraction of global food demand. We find seaweed can be grown in tropical oceans, even after nuclear war. The simulated growth is high enough to allow a scale up to an equivalent of 70 % of the global human caloric demand (spread among food, animal feed, and biofuels) in around 7 to 16 months, while only using a small fraction of the global ocean area. The results also show that the growth of seaweed increases with the severity of the nuclear war, as more nutrients become available due to increased vertical mixing. This means that seaweed has the potential to be a viable resilient food source for abrupt sunlight reduction scenarios.

Significance Statement

Cooling in abrupt sunlight reduction scenarios (ASRSs) such as nuclear winter will make agriculture, as it is practiced today, untenable. We therefore need resilient foods that can still produce yield in such an environment. This study calculates that seaweed will grow after a nuclear war and its production can be quickly scaled up to provide a significant contribution to global food security.

Abrupt sunlight reduction scenarios as a risk to global food security

How can we avoid a global famine if Earth's surface is suddenly receiving significantly less sunlight? The main mechanisms to cause such a reduction of sunlight are either nuclear war (1, 2), asteroid/comet impacts (3, 4) or large volcanic eruptions (5, 6). Those three mechanisms are grouped together as abrupt sunlight reduction scenarios (ASRSs). These scenarios could lead to a massive injection of particles into the upper atmosphere, where they have long residence times, limiting sunlight reaching the Earth's surface, in turn disrupting global climate and causing a significant drop in temperature. For example, after a large nuclear war, global temperature could drop up to 9°C below current values (1, 7). In the historical and paleo records, large volcanic eruptions lead to reductions of global average temperature on the order of 1°C (8, 9), with higher reductions on land and in the Northern Hemisphere, leading to famines, disease outbreaks, political instability, and regime changes (10).

Extreme changes in temperature due to nuclear winter might reduce currently practiced agriculture by about 90% if no extensive precautions and adaptations are taken (11). The effects of ASRSs scale with the size of the impacting event, but it is established that even smaller events like a regional nuclear war could have a large negative impact (12, 13) in both combatant and non-combatant countries (14). Therefore, a much larger effect can be expected for a full-scale

nuclear war and other large ASRSs. The effects would differ strongly between countries, due to differences in national food production and storage, as well as spatially heterogeneous effects of the ASRS on the climate (1, 15).

If such an ASRS event occurred today, it would hit a largely unprepared world. Wheat is the most widely stored food, and global storage would only last for a few months at current consumption (16), while the cool climate after an ASRS can persist from years to over a decade (1, 5, 7). Other sources of food including wild captured fish could decrease quickly, especially if they are not managed sustainably before the ASRS (17). This means that alternative food sources are needed to avoid a global famine. They need to reliably produce food over several years, even if there is less sunlight available, and the temperature is lower. We will refer to these as resilient foods in the following.

Why seaweed?

Recent years have seen a constant increase in the research on resilient foods (18, 19), especially for ASRSs (20, 21). Resilient food solutions include leaf protein concentrate (22), greenhouse crop production (23), single cell protein from natural gas (24) and hydrogen (25), sugar from lignocellulosic biomass (26), synthetic fat from petroleum (27), and wild edible plants (19). In combination, these resilient food solutions could provide enough calories to avoid anyone starving after the nuclear war scenario (15). However, many of the resilient foods are in a very early stage of technological development. It would be difficult to ramp up production on very short notice to produce enough food to avoid a global famine. Other well-developed resilient foods are needed that can be used in low tech settings.

One promising candidate is seaweed (18, 21). It is fast growing and highly scalable (28, 29), and has been highlighted as a valuable addition to the global food supply by the FAO for decades (30–32), since it is not competing with conventional agriculture when it comes to freshwater, land, fertilizers or pesticides (33). It also has been an important part of human food for millennia and was used in its dried form for long voyages hundreds of years ago (34). Seaweed gives good yields even in low tech settings (28). In addition, a nuclear conflict and large volcanic eruptions will likely lead to a higher intensity of UV radiation at the Earth's surface, as the ozone layer could be depleted (35–37). In comparison to land-based agriculture, seaweed is partly shielded from this by the water it grows in. Moreover, seaweed is a potential biofuel solution (29, 38). Recent research established that seaweed could contribute up to 100 % of the human protein need (39) and that globally around 48 million km² are suitable for seaweed production (40). However, the places best suited for seaweed production today are likely to differ in an ASRS, due to changes in temperature and nutrient availability caused by changes in climate and the ocean state(41).

This paper aims to establish where and how well seaweed would grow in an ASRS. We base this on nuclear winter Earth system simulations, as this kind of ASRS has been studied most, and detailed datasets are available (1, 41). To evaluate the feasibility of seaweed as a resilient food we use a global, empirical seaweed growth model based on *Gracilaria tikvahiae* (42, 43), which is used for human consumption (44), is grown globally (e.g. in Brazil and China) (45) and shows

growth behavior and resource needs in the range of many other seaweed (46). This model uses nuclear winter ocean simulation and calculates the fraction of the optimal growth rate for seaweed based on factors for nutrients, salinity, temperature and illumination. This total growth factor is the product of those factors. The second aim is to explore how quickly seaweed can be scaled up to meet an equivalent 70% of the global human caloric need, as this would be enough seaweed to contribute to both food and animal feed, while not risking iodine poisoning, and still having enough seaweed to keep current biofuel production running. This scale-up calculation is based on the growth rates from the seaweed growth model. Taken together, this will evaluate the feasibility of seaweed as a resilient food in an ASRS.

Growing seaweed after nuclear war

Running the seaweed growth model for the first ten years after nuclear war calculates seaweed growth rate for all oceans globally. Looking at those growth rates in aggregate has two clear results (Figure 1). First, that seaweed growth rate is directly proportional to nuclear war severity, with faster growth under more extreme forcing. Second, the growth of seaweed is fastest at the beginning of the ten years (with a peak at year two) and slows down over time. This seems counterintuitive, as one would expect that seaweed growth would be more limited the more climate is impacted. However, the main factor to limit growth is not temperature or illumination, but nutrients (Figure 2). The ocean surface is generally nutrient poor. This changes after a nuclear war, as global ocean circulation patterns are disrupted and nutrients are brought to the surface due to increased vertical mixing during the cooling event, creating a new ocean state with enhanced surface macronutrients that lasts for decades (41). This vertical mixing process is proportional to the severity of the nuclear war (41), which in turn leads to the improved seaweed growth after more severe nuclear wars.

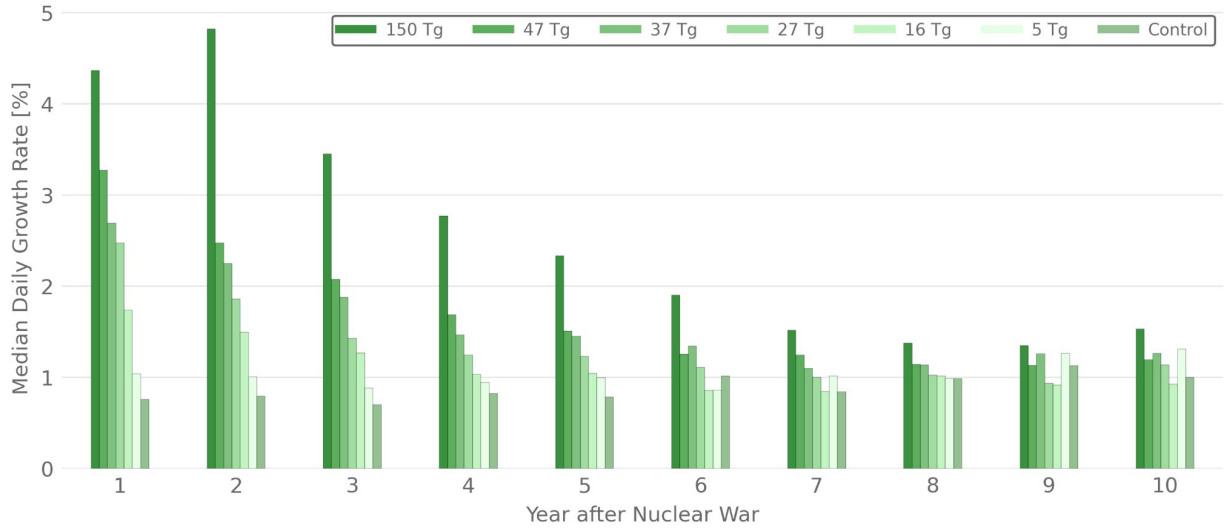


Figure 1: Comparison of global median daily seaweed growth after nuclear war of different magnitude and a control run. Colors indicate the severity of the nuclear war in teragrams

soot ejected. Control is a scenario without soot injection. Growth rates shown only include areas between -45° to +45° of latitude, as the areas north and south of this are unsuitable for *Gracilaria tikvahiae* even before the nuclear war. Grey bar indicates the range of the results of the control run to show the variability of the model without a soot injection.

The following results and discussion will focus on the US-Russia 150 Tg (trillion grams = million tons) of soot scenario, as in such a case seaweed is most important as an addition to food security, while also having the highest growth. There are three distinct growth regimes determined using k-means clustering, which groups regions (Figure 3) together that have a similar growth pattern over time (Figure 2). In the following, we describe the differences in cluster behavior and location:

- Cluster 1 (Fig 2 left panels): This cluster is unsuited for *Gracilaria tikvahiae* before the nuclear war, due to limited nutrients. This changes shortly after the onset of the cooling event (Fig 2d) as nutrient limitation decreases and thus the seaweed can grow faster. This effect continues throughout the nuclear winter, but becomes more seasonal and weaker over time. After the first 1-2 years, this nutrient effect is countered by increased temperature limitation as the ocean cools (Figure 2j), leading to overall declining growth. Also, the growth declines after the third year even more, due to increased nutrient limitation, though this varies regionally, with some portions of the cluster (lighter green) having relieved nutrient stress and elevated growth after more than 100 months (Figure 2m). This cluster can be found globally near the equator ± 30° latitude and covers one third of the global ocean area (Figure 3).
- Cluster 2 (Figure 2 center panels): This cluster is characterized by its very low overall total growth factor (Figure 2n). The median growth factor is close to zero for the entire 10 years of the time series. However, different regions in this cluster are growth limited for different reasons. While a large portion of the regions are limited by being located in very high or very low latitudes and thus in water too cold and dark to grow seaweed, another portion is located in warm, but nutrient poor environments closer to the equator and marginal seas where the ocean model does not simulate nutrient dynamics well (Figure 3). These regions are nutrient poor, due to little exchange of water with other parts of the ocean. However, this might also be partly an artifact of the resolution of the forcing simulated data, as this area is only represented by few data points, and nutrients from rivers are not included. Cluster 2 accounts roughly for half of the global ocean area.
- Cluster 3 (Figure 2 right panels): The regions in this cluster show the highest overall growth factor, with an average of almost half of the optimal growth rate (Figure 2o). They are also very suitable for seaweed even before a nuclear war. Still, those regions experience a drop in their productivity after the nuclear war. The overall growth factor declines slowly for the first 6-7 years, before it starts to rise again. This drop is driven by declining temperature and declining nutrient availability (Figure 2f, 2l). The temperature reaches its pre-war values after 5-6 years, while the nutrients follow 1-2 years after that. After recovery, the nutrients even reach values higher than during the pre-war period. Most of the regions with this growth pattern are located in the Pacific Ocean and far away from human settlements (Figure 3). Still, there are several areas with this growth pattern that

are located near coasts (e.g. in Chile and Peru). It covers 13 % of the global ocean area. In addition, there are also occurrences of this growth pattern where major rivers meet the ocean (e.g. Ganges Delta, Bight of Biafra, Senegal River Delta). The cluster is strongly influenced by the so-called Nuclear Niño (47). This means that the shift in ocean currents due to the nuclear winter creates El Niño like weather and ocean conditions for several years with warmer water in much of the ocean west of Central America. Finally, this cluster partly overlaps with the regions that have been identified as being best for low cost, large scale seaweed farming (48).

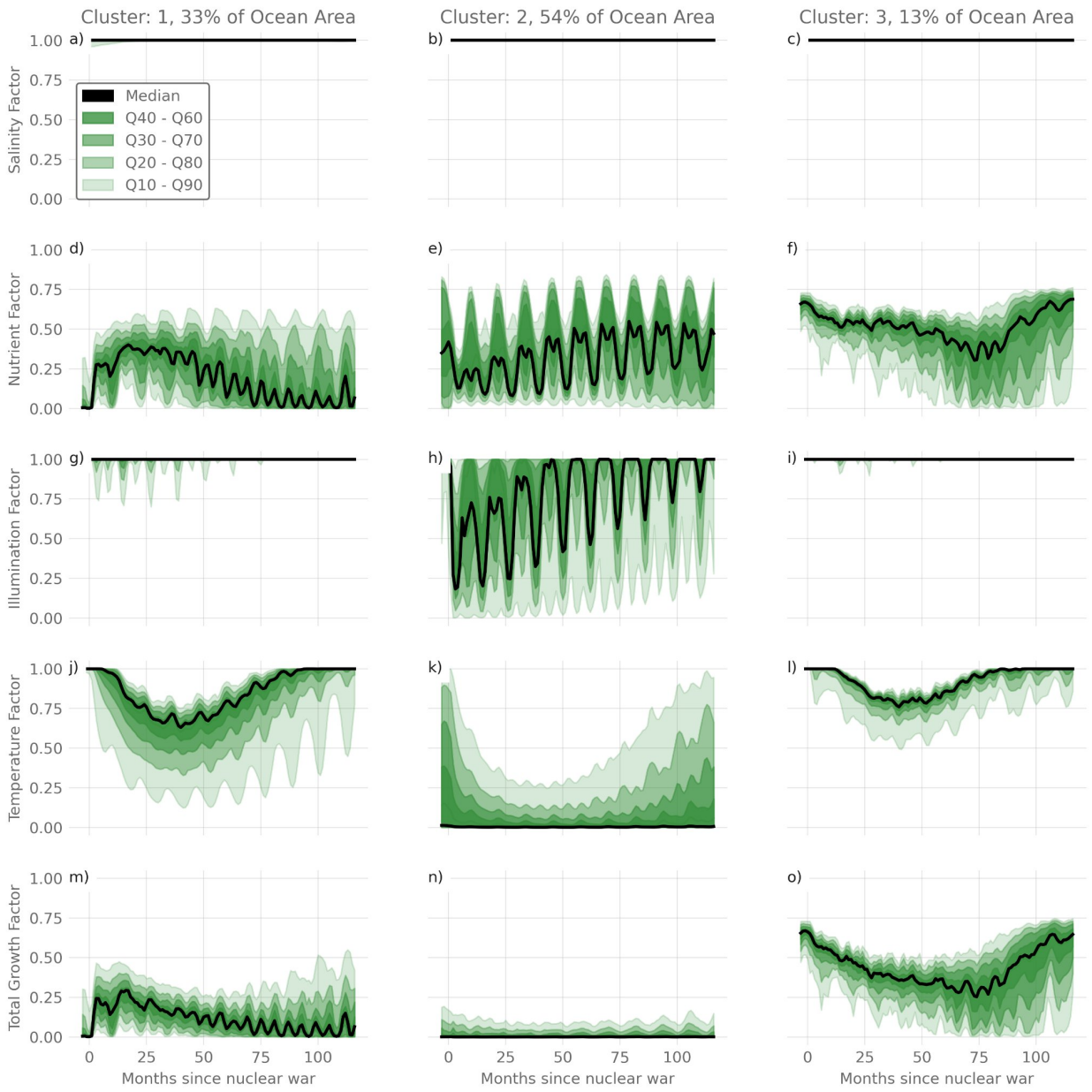


Figure 2: Time series of the growth factors (salinity, nutrients, illumination, temperature) for the three *Gracilaria tikvahiae* growth regime clusters and the overall total growth factor (which is the product of the four factors). The black line indicates the median in the cluster. Q refers to quantiles. Green shaded areas show how much of all the time series of the cluster is contained within the range. The darkest green contains the 20% of the time series that are closest to the median, while the next shade of green contains 40 %, up to a value of 80 % of the dataset for the lightest green. All calculations are weighted by area of covered ocean regions.

Overall, cluster 1 and especially cluster 3 are most suited for seaweed cultivation after nuclear war, while cluster 2 should be mostly avoided. Additional figures showing the seaweed growth patterns for a selection of large marine ecosystems (Figure S1, S2) and an example of the global distribution of growth rates (Figure S3-S5) can be found in the supplementary information . Our results highlight that the main factors for reduced growth are nutrients and to a lesser extent temperature.

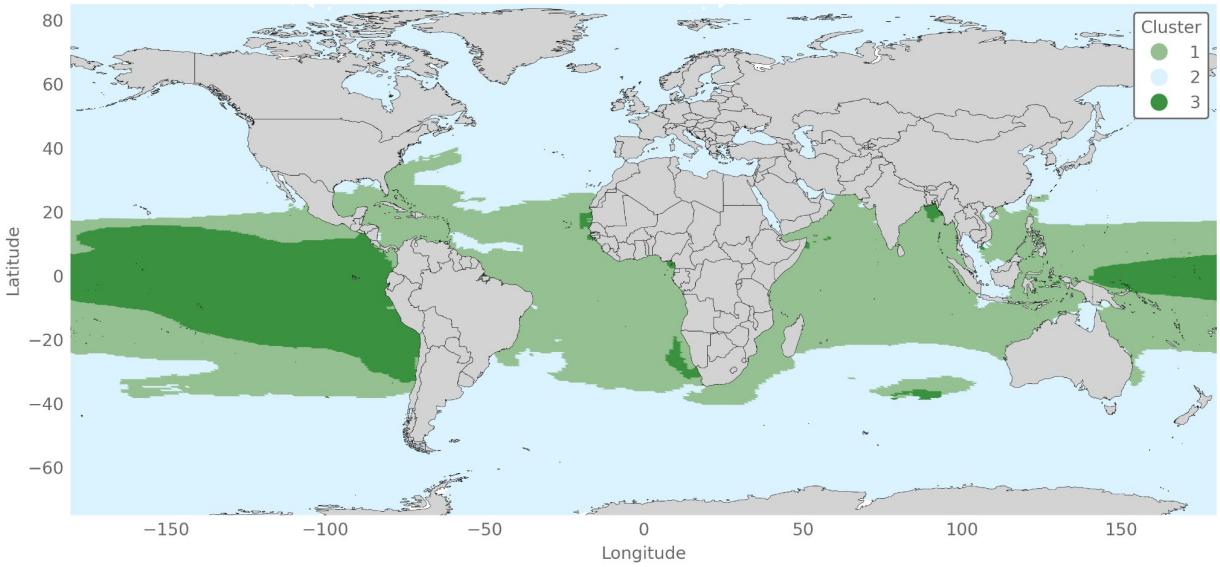


Figure 3: Global locations of the *Gracilaria tikvahiae* growth regime clusters for a 150 Tg nuclear war scenario. Colors indicate the different clusters. White areas indicate missing data.

Scaling up of seaweed production

After calculating the growth rates after nuclear war, we use a scale-up model to calculate how quickly seaweed farming can be scaled up to a level needed to produce an equivalent of 70 % of the global human food demand. The model assumes that seaweed farms are built until the area needed to fulfill 70 % of the global human food demand can be satisfied on average over the 10 years of the simulation. The yield is used to stock existing farms until those are saturated. Thereafter, all yield is used for food, feed and biofuel. This is under the assumption that enough other food resources are available until the seaweed is scaled up and therefore seaweed can only be distributed for consumption once the target yield is reached (15). This way the overall availability of food for the years after the nuclear war is maximized.

The model assumes an initial global seaweed stock of 10,000 t on an area of 100 km². Currently, around 35,000,000 t of seaweed are produced annually (45) on an area of around 1,600 km² (49). This means the starting parameters of the model are considerably less than the area used and amount produced today, and were chosen to have a conservative estimate that reflects the

possible disruptions by a nuclear war. This includes inability to grow tropical seaweed species after nuclear war and transporting suitable seaweed species to their new growing areas.

Cluster 2 has such a low overall growth rate that it is excluded from further analysis, as it would be ineffective to grow seaweed there. Clusters 1 and 3 are productive enough to produce enough seaweed to satisfy 70 % of global caloric demand on average over the entire 10 years of the ASRS event(Figure 4). However, the clusters differ considerably in how quickly they can provide seaweed, when they have their peak productivity and how much growing area is needed.

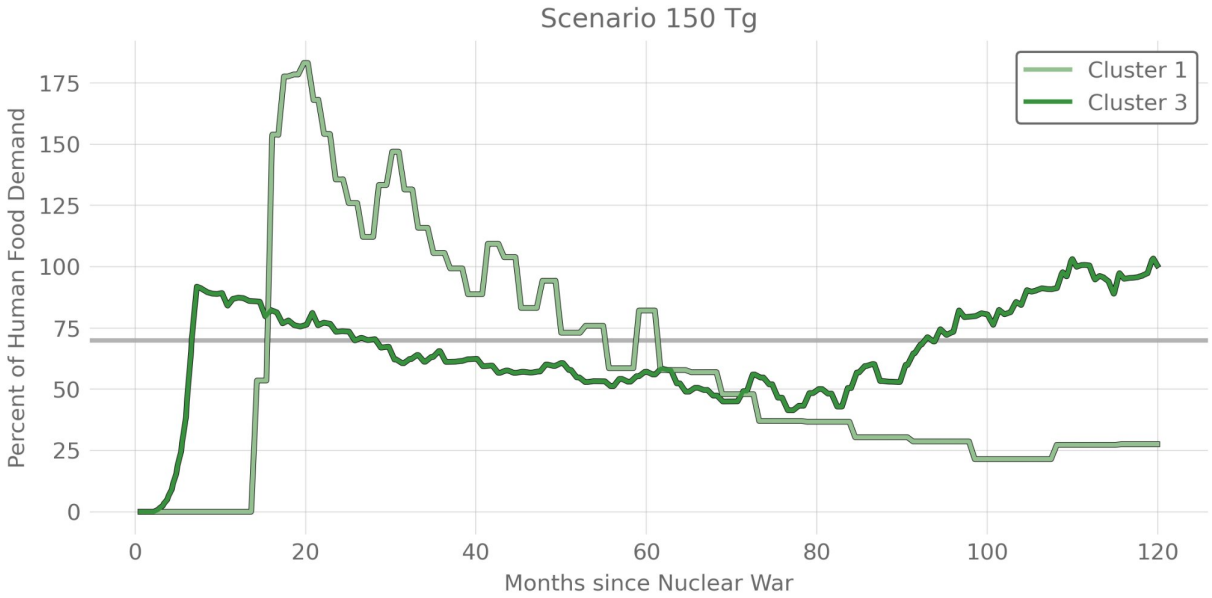


Figure 4: Seaweed production as percent of human food demand for suitable seaweed growth clusters (150 Tg nuclear war scenario and 30 % per day as optimal growth rate). This is optimized for meeting an equivalent of 70 % of the global human caloric demand on average for the whole 10 years (gray line).

Cluster 1 is the least productive of the viable clusters suited for seaweed production. Due to its lower productivity it takes considerably longer to reach saturation and produce yields (~16 months; Figure 4). Also it needs a very large area (247,000 km²), as the growth rates decline over time. It still might be a worthwhile investment to create seaweed farms here, as many countries only have this cluster available (e.g. Australia, United States) and it allows food production in the first few years of the nuclear winter, when food security is most under threat (50). Given a seaweed water content of 11 % (51) this results in an average yield of 8.7 tons dry/year/hectare for cluster 1 (median growth rate 3.3 % per day).

As cluster 3 is located in highly productive areas, it can be quickly scaled up, with daily growth rates reaching 50 % (and above) of the optimum around half of the time (Figure 2). Thus, after around 7 months, enough seaweed is grown that it can be used to feed people instead of saturating new seaweed farms. Due to this high yield, only around 63,000 km² of ocean are needed to produce the seaweed with this cluster, which is about the size of Lithuania. In comparison, the exclusive economic zone of Peru alone, which consists mostly of cluster 3 has

a total size of around 900,000 km², of which a considerable fraction has shallow depths and thus allows low-tech seaweed farming (though not all is near ports), while also being a low cost area for seaweed production (48). This means that enough area is available to grow seaweed on such a global scale. Given a seaweed water content of 11 % (51) this results in an average yield of 33.99 tons dry/year/hectare for cluster 3 (median growth rate 13.3 % per day).

Potential challenges and their implications

Scaling up seaweed farm infrastructure

Our study demonstrates that seaweed can play a significant role in meeting human food demands following a severe nuclear war. Our findings indicate that a scaled-up seaweed production of 70% of human food demand is possible in as much as 7 months. However, the results also show that the global median of seaweed growth is smaller in less severe nuclear exchanges, as fewer nutrients reach the surface waters of the ocean, limiting seaweed growth (Figure 1). However, this does not mean that scale-up will be slower in those cases (Figure S6), as in all nuclear war scenarios there are wide areas in the oceans with high growth rates. The limiting factor is the speed of the global scaleup in the construction of new seaweed farms and not the growth rate. For the more severe scenarios a slightly longer scale-up is needed, to account for the fact that the growth rate experiences a lower dip in year three, which was to be compensated with a bigger area. Still, this means that seaweed could be a viable addition to global food security now and in severe ASRSs, but also in smaller nuclear exchanges and volcanic eruptions.

To fully take advantage of the fast growing seaweed, hundreds of km² of seaweed farms would have to be built each day. However, seaweed farms can be quite low tech and still provide good yields (28) (Figure S7). It also has been proposed to build 100 km² floatable seaweed rafts (52). If those could be mass produced it would be possible to cover even much more area per day, thus allowing production of even more seaweed than proposed here. The creation of those seaweed farms would be a global priority in the case of nuclear war. Therefore, it seems possible to create farms of this magnitude, especially as past work has shown that there are enough resources to scale up greenhouse production by a larger amount than needed for seaweed farms here (23). Analysis of the scale up of the infrastructure is beyond the scope of this paper, but will need to be studied in future research.

With decreasing productivity the seaweed needs increasingly large areas to meet a production equivalent to 70 % of global human food demand. Still, the 178,000 km² needed for the less productive areas are a very small fraction of the global ocean area. A recent study showed that this is also the same magnitude of area needed to sequester a gigaton of Carbon from the atmosphere (48). The United States alone has coastal waters not further than 2.5 km from the coastline or 50 km from a harbor of around 145,000 km². Those coastal waters are suitable for relatively low tech seaweed farms (28, 53). This means that even in the case that seaweed production is much more unproductive than estimated here, globally there are much larger areas available for growing seaweed than are needed in even the most pessimistic cases. Still, the

results show that areas that are currently seen as resilient in a nuclear winter like New Zealand (54) will not be able to further improve their resilience with seaweed, as their coastal waters are either too cold or nutrient poor.

The seaweed farm design in this study assumes a very low tech approach, which mainly consists of ropes that are kept in place by anchors and buoys (28, 53). This is done to assess the feasibility of seaweed production after nuclear war under the worst conditions. However, this also means that higher yields and lower labor requirements could be accomplished by using more modern, offshore approaches to seaweed production (55). This also opens up the possibility to grow more of the seaweed in cluster 3, to ensure the highest growth rates possible. As such, productive offshore cultivation is possible with current and near-future technologies (56); however, such high tech solutions may not be accessible to all in an ASRS. Therefore, low-tech options such as small scale vessels for transport are a viable alternative, as more people have the skills to use them and they have lower energy requirements.

Nutrient availability for seaweed growth

In many regions of the ocean net primary production is strongly limited by iron availability, both before and after a nuclear war (41). However, the research on this is mainly based on phytoplankton and not on seaweed (e.g. (57)). While there is some evidence that seaweed growth can be inhibited by iron deficiency (58), this does not seem to be a major limiting factor. Iron is mainly needed for the reduction of nitrate (59). Therefore, if the nitrogen is available as ammonium, seaweed can also grow in iron sparse environments. The seaweed growth model considers ammonium, nitrate and phosphate and limits the growth with the nutrient that is least available. In the case of this study, ammonium is usually the limiting factor (Figure S8). Still, the ammonium is enough to support the growth rates shown here. This also means that the growth rates could be further enhanced by making more iron available, as this would allow the seaweed to also use nitrate. Therefore, iron fertilization might be a good way to increase growth rates further. Such large scale ocean fertilization with iron would be an unprecedented project, yet it has also been proposed as a climate change solution (60). Therefore, research into potential ocean fertilization could both help mitigate risks from climate change and nuclear winter.

Potential problems of seaweed consumption

Seaweed can have high concentrations of essential elements such as iodine and heavy metals such as arsenic, which are associated with health risks (61). The United States defines the tolerable upper intake level of iodine for almost all individuals as 1.1 mg per day. However, other countries with a diet richer in iodine tolerate higher limits (e.g. Japan (62)). There has also been research showing that humans can tolerate extremely high levels of iodine of around 50 mg per day for a prolonged period of time, without suffering permanent damage (63). This means that, at least for a few months, high iodine levels in the food due to a large intake of seaweed could be tolerable. Also, iodine concentration in seaweed varies considerably and changes with season, location, preparation and species (64, 65). Therefore, iodine concentrations and other potentially harmful substances would have to be monitored.

Radioactive fallout, that is, the deposition of radionuclides, is characterized by uneven distribution, which highly depends on scale of and targets in a nuclear war. Radionuclide concentration and behavior has been explored in some depth in the aftermath of events such as the Fukushima nuclear accident (66). The main risks come from consuming fish, as those accumulate environmental contaminants. However, it remains unclear how the much larger emission of radioactive particles during a nuclear war would play out. Continuous surveillance will be necessary to define high-risk foods. One particular concern is the fact that seaweeds tend to be high in iodine, and radioactive iodine could be incorporated instead. However, since the half-life is only hours to days (depending on the isotope) (67), it should not be a significant problem as the seaweed needs to be scaled up first and would only be consumed after several months.

Harvest and preparation for consumption

The seaweed scale-up model assumes a constant loss of 20 % of yields to grazers such as fish, epiphytes (plants growing on the seaweed) and diseases. This is the upper bound commonly found in marine fisheries (68). However, values in extremely large seaweed farming might differ considerably. Therefore, adaptations will have to be made to ensure healthy conditions for seaweed. One promising way to ensure this is seaweed diversification (69). This simply means that seaweed should not be grown in monoculture.

It is unclear which seaweed species would be overall best suited for food production after a nuclear war. However, it is likely that a variety of different seaweed species could be used to make food production more resilient, adapt it to the local environment, and provide diet diversity. Still, this work makes a contribution to our understanding of food production after nuclear war, as it shows how much seaweed production will shift due to the changed climatic conditions. Species selection must focus on how well they cope with potential environmental stressors including low temperature, nutrients, grazing pressure and pathogens. In addition, this selection of seaweed species can be used to optimize the nutrient content (e.g. making sure that enough fat and protein is available).

Seaweed spoils quickly once harvested. Therefore, most of it has to be preserved to get it to consumers. There are a variety of preservation methods including salting, canning, freezing and drying. Drying has the further advantage of reducing shipping mass and cost. Currently, seaweed is often dried by solar drying (70). However, this will generally not be feasible in the colder, higher relative humidity, lower sunlight conditions of nuclear winter. While seaweed can also be dried by freeze drying, vacuum drying and convective air drying (64), none of these techniques have been used to dry seaweed on the scale needed after nuclear war. Therefore, additional research is needed to demonstrate the feasibility in this condition.

Preparations to ensure successful seaweed production after a nuclear war

The challenges that have to be overcome to produce seaweed on such a large scale as proposed in this paper are considerable. However, there is also much that could be done today to elevate the chances of success:

- In many seaweed farm designs, seaweed is either inserted into twisted rope by hand or seaweed spores are allowed to grow on seedling lines in so-called hatcheries (28, 71). The latter is more efficient, but needs some infrastructure set up in preparation. The infrastructure to allow this could be deployed in regions that would have high seaweed growth rates after nuclear war.
- Creating such a large number of seaweed farms will likely consume a considerable amount of working hours and materials. If plans are made beforehand that outline how this can be accomplished, the response would be quicker.
- This study focuses on *Gracilaria tikvahiae*, because it has an empirical growth model available (72). It is likely that successful food production with seaweed in an ASRS needs a wider variety of species. This means there is a need to model additional species, so that the best species combination for every region can be identified.
- Iodine is the main limiting factor when it comes to using seaweed for human consumption. However, the amount of iodine in seaweed varies strongly depending on species, preparation and environmental factors. If the amount of iodine could be reduced cost-effectively, more humans and animals could be fed with seaweed.
- The ocean model used has a resolution of ~1°. This means that marginal seas like the Red Sea cannot be modeled in a sufficient resolution. If data with a finer resolution becomes available this study could be repeated to discover how suitable marginal seas are for seaweed production after nuclear war.
- Seaweed is not only a good source of food after nuclear war, but also now (32). This means that food security could be improved both today and after nuclear war, if seaweed would be used more today. This would also improve the pool of skilled labor and improve the technology available. Especially promising are places that have a high productivity both now and after nuclear war (e.g. west coast of South America).
- There are also calls to action to use seaweed as a way to sequester carbon from the atmosphere to combat climate change (39). A recent global analysis has identified a suitable global ocean area of 48 million km² suitable for seaweed production (40). Even if only a fraction of this potential would be realized this would provide both climate change benefits and increase civilizational resilience in ASRSs.

Conclusion

Seaweed has a high potential to be an important pillar of global food security. Not only now, but also after a nuclear war. This study shows that, especially in the case of a severe nuclear war, large ocean areas exist that have high growth rates. Partly, these are also located in areas where seaweed production is feasible today, highlighting important areas to facilitate seaweed

production now. Given enough preparation and using the most productive areas available, seaweed could produce an equivalent of 70 % of global human caloric needs after only 7 months. While a pure seaweed diet is not possible, this intervention would have an expected value of averting ~1.2 billion deaths from starvation (15 % of human food demand times 8 billion people). The main bottleneck to produce enough seaweed to make a significant contribution to global food security is the speed at which the construction of new seaweed farms can be scaled up. Therefore, investments into increasing such capacity would help to avoid a global famine in an ASRS. In addition, global carbon sequestration with seaweed has a similar demand in inputs as the scale proposed here to use seaweed as a resilient food after a nuclear war (48). This means that seaweed farming at 30 times the scale of today would combat climate change, while also making the food system much more resilient in ASRSs.

Methods

The analysis in this paper is done in a two step approach (Figure 5). First, we use an empirical seaweed model to calculate global seaweed growth after nuclear war. Second, we use the resulting growth rates to calculate how quickly global seaweed production can be scaled up to meet 70 % of the global caloric need.

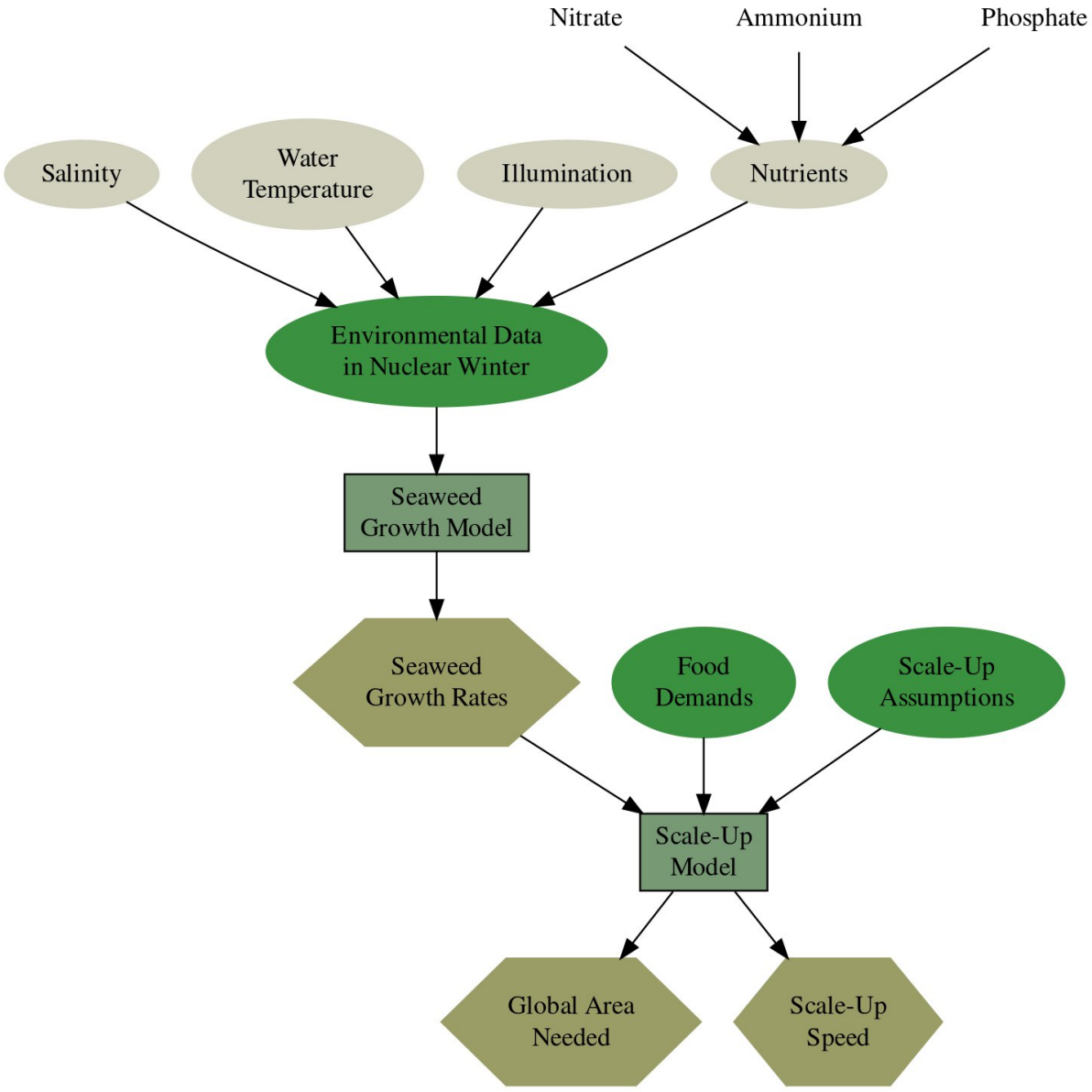


Figure 5: Workflow for modeling set-up and simulation. The seaweed growth model calculates seaweed growth rates based on nuclear winter environmental simulation. Based on those growth rates, the scale-up model estimates how quickly 70 % of the global caloric demand could be satisfied with seaweed and how much area would be needed for this. Hexagons highlight resulting data, ellipses inputs (forcing and assumptions) and squares the models.

Seaweed Species Selection for Modelling

Seaweeds exhibit a wide range in their properties including morphology, nutrient content and their preferred environmental conditions. A seaweed species was chosen that would be successful in the conditions of a nuclear winter. The growth model is based on the species *Gracilaria tikvahiae* (42, 43), a morphologically variable red macrophytic algae (*Rhodophyta*)

(Figure S9). It is commonly found in the Atlantic estuarine environments and the Western North Atlantic Ocean, with extremes of its geographic range may be found in the environmental regimes of Canada and southern Mexico (73).

Gracilaria tikvahiae was chosen for its persistence in the vegetative condition so that it can be continuously trimmed as well as its growth rate and dry weight yield (43) under a wide variety of environmental conditions, is used for human consumption (44) and is grown commercially in countries around the world (e.g. China, Brazil and Monaco) (45). Its current growing conditions are similar to those found near the equator in the case of nuclear winter (41) and its environmental constraints for growth are well known (72). It has also been proven to be suitable for offshore cultivation (38). It has growth rates, as well as nutrient, illumination and temperature needs which are in a typical range for seaweeds (46, 74).

Seaweed Growth Model

The analysis to assess the feasibility of seaweed as a resilient food source is split into two steps (Figure 5). First, we calculate the growth rate of the seaweed on a global scale. To do this we use the empirical model for the growth of *Gracilaria tikvahiae* based on James and Boriah (72). The model uses growth limitations. It starts with the optimal growth rate of 30 % per day, which is conservative (75, 76), as cases with up to 60 % per day have been reported in controlled experiments for *Gracilaria tikvahiae* (43). The optimal growth rate is multiplied by limiting factors for illumination, temperature, nutrients, salinity and self-shading, which results in the actual growth rate. For a detailed description of the factors see the Figure S10-S14. The code (77) and data (78) for the growth model can be found at the corresponding repositories. We excluded the self-shading factor in our adaptation of the growth model and only looked at it in the scale-up model, as it is more relevant for continuous harvesting and less so for assessing if seaweed can grow after nuclear war at all. This means that in the scale-up model, the seaweed is regularly harvested to maximize yield subject to a reasonable harvest frequency.

The growth model uses as its forcing Earth system model simulation (1, 41), which models the impact of a range of nuclear wars on the global ocean state. This ocean model simulation component contains information about salinity, sea surface temperature, illumination, and nutrients (ammonium, nitrate, phosphate). The original dataset reflects the effects of a nuclear war on the atmosphere and oceans. The scenarios consists of soot injections of 5, 16, 27, 37, 47 and 150 Tg of soot into the atmosphere and a control run. The ocean model has a resolution of ~1° grid cells. Due to this resolution, processes near coasts underestimate nutrient fluxes and thus overall productivity near coasts. We model the first ten years after a nuclear war, as after those ten years conventional agriculture largely recovers (1).

When the seaweed model is run, it results in a time series for all the growth factors and the total growth factor, for each grid cell in the ocean. The total growth factor is simply the product of the single growth factors. To find patterns in the total growth factors between different grid cells, we clustered the time series of the total growth factor using k-means clustering with dynamic time warping (79) as the distance measure, as implemented in tslearn (80). Dynamic time warping

allows the similarity of two time series to be detected, even if they happen at different speeds. In the case of this paper, two regions will be counted in the same cluster if they have the same overall growth pattern, even if the pattern is slightly shifted in both timing and amplitude. The optimal number of clusters was determined by using the elbow method (Figure S15) and resulted in three distinct clusters, which represent the main growth regimes in seaweed that can be found after nuclear war.

Seaweed Scale-Up Model

The second step in our analysis is a scale-up model (81). This model uses the modeled seaweed growth rates to calculate how quickly society could scale up global seaweed production to account for an equivalent 70 % of global human caloric demand. This would be enough to substitute 15 % of human food by seaweed, 10 % of animal feed and 100 % of the global biofuel production (though it may not be feasible for seaweed to provide bio diesel, the conversion of efficiency of seaweed to ethanol may be lower than that for grains, necessitating a greater seaweed supply (82)). While it seems to be possible to feed humans iodine in levels that account for roughly 20 % of the food from seaweed (63), this results in health problems. We therefore settled to 15 % for food to have a wider safety margin. Similar, but possibly stricter limits can be found in animals (83). However, there are also reports of animals being fed almost exclusively seaweed (84), so the limits used in this study are on the cautious side.

The model scales up the seaweed in such a way that over the whole time period of ten years 70 % of global calories can be produced on average. The amount of new seaweed farms built each day is represented by a logistic curve (Figure S16), which models the scale-up of seaweed farm production by comparing it to the scale-up of aircraft production in World War II in the United States (85). In each time step the model grows the seaweed by using the modeled seaweed growth rate for that day. This accounts for self-shading (72) (Figure S14) and how much area is available to grow seaweed. The seaweed grows until it has reached a density of 3.6 kg per m^2 and is then cut back to 1.2 kg per m^2, the optimal trimming threshold to minimize self-shading (38, 43). Once the whole seaweed farm area is saturated with seaweed, all yield thereafter can be used to produce food, feed and biofuel. This is based on a low tech seaweed farm design. Such designs consist mainly of seedling lines to attach the seaweed, longlines to attach the seedling lines, buoyant to keep the longlines afloat and anchors to fix the farm in place (28). See (53) for a selection of low tech seaweed farm design schematics.

Seaweed farm building scale-up

To estimate how quickly seaweed farms could be built, we mainly looked at rope production, as this is the main component and most complex part of low-tech seaweed farming (28). The other main components being anchors and buoys, which can be substituted through rocks and black plastic bottles (86). Currently 60.5 million tonnes of polyester fibers are produced per year (87), Out of this synthetic fiber category at least polyamide (Nylon), polypropylene and polyethylene are suitable for seaweed farms. Conservatively, we are assuming no additional scale-up of fiber

production and that only 50 million tonnes of global polyester production are suitable for seaweed farms. Given the 2 types of ropes (0.025 kg/m for seedling lines and 0.11 kg/m for longlines) in the farm design 33.9 tons of suitable rope are needed to create 1 km² of seaweed farm in a low tech setting. This means that around 4000 km² of seaweed farms can be built per day with current global fiber production. However, the current production of ropes is much lower than that and will need to be scaled up. To estimate the possible speed of this scale-up we use the switch of the American automobile industry to producing aircraft (and other war machinery outputs) in the Second World War (85). This shows that a considerable scale up can be done in around 9 months. To finally estimate the seaweed farm production over time, we use the scale up speed from the Second World War with 4000 km² as the maximum production and fit a logistic growth curve to it (Figure S12).

We further assume that the distribution and installation of the seaweed farms will be possible if the needed amount of rope will be provided. Overall, the seaweed farm production is a considerably smaller effort than the American war effort in World War Two alone, and should thus be possible to accomplish now as well.

Acknowledgements

The authors would like to thank Scott Carlton James (Baylor University), who helped with the initial scoping of the project by running some of the ocean model data through his growth model and providing said growth model to the project, but passed away in 2021. He was a friendly and encouraging person who was quick to assist if questions arose. The authors would also like to thank their colleagues at the Alliance to Feed the Earth in Disasters (ALLFED), Noah Wescombe, Morgan Rivers, Kevin Rassool, Inès Jimenez and Sahil Shah for their continuous support and guidance throughout the research process. Moreover, technical assistance from the Harrison Lab (especially Victoria Garza) of the Louisiana State University has been instrumental to the completion of this manuscript. We would further like to thank Rene Recktenwald and Liza Vabistsevits for helping improve the clarity and usability of the code created for this project. Finally, we would like to thank Patrick Mineault for setting up the Good Research Code Handbook (88). The insights gained from it considerably improved the code for this paper.

Funding Sources

This work was funded by the Alliance to Feed the Earth in Disasters (ALLFED). CSH was supported by Open Philanthropy, NOAA CPO, and NSF awards #2218777 and #2149890.

References

1. J. Coupe, C. G. Bardeen, A. Robock, O. B. Toon, Nuclear Winter Responses to Nuclear War Between the United States and Russia in the Whole Atmosphere Community Climate Model Version 4 and the Goddard Institute for Space Studies ModelE. *Journal of Geophysical Research: Atmospheres* **124**, 8522–8543 (2019).
2. O. B. Toon, A. Robock, R. P. Turco, Environmental consequences of nuclear war. *Physics today* **61**, 37 (2008).

3. C. R. Chapman, D. Morrison, Impacts on the Earth by asteroids and comets: assessing the hazard. *Nature* **367**, 33–40 (1994).
4. C. R. Tabor, C. G. Bardeen, B. L. Otto-Bliesner, R. R. Garcia, O. B. Toon, Causes and Climatic Consequences of the Impact Winter at the Cretaceous-Paleogene Boundary. *Geophysical Research Letters* **47**, e60121 (2020).
5. M. R. Rampino, Supereruptions as a Threat to Civilizations on Earth-like Planets. *Icarus* **156**, 562–569 (2002).
6. J. Rougier, R. S. J. Sparks, K. V. Cashman, S. K. Brown, The global magnitude–frequency relationship for large explosive volcanic eruptions. *Earth and Planetary Science Letters* **482**, 621–629 (2018).
7. R. P. Turco, O. B. Toon, T. P. Ackerman, J. B. Pollack, C. Sagan, Nuclear Winter: Global Consequences of Multiple Nuclear Explosions. *Science* **222**, 1283–1292 (1983).
8. M. Sigl, *et al.*, Timing and climate forcing of volcanic eruptions for the past 2,500 years. *Nature* **523**, 543–549 (2015).
9. B. L. Otto-Bliesner, *et al.*, Climate Variability and Change since 850 CE: An Ensemble Approach with the Community Earth System Model. *Bulletin of the American Meteorological Society* **97**, 735–754 (2016).
10. S. White, *The climate of rebellion in the early modern Ottoman Empire* (Cambridge University Press, 2013).
11. L. Xia, *et al.*, Global food insecurity and famine from reduced crop, marine fishery and livestock production due to climate disruption from nuclear war soot injection. *Nat Food* **3**, 586–596 (2022).
12. M. J. Mills, O. B. Toon, J. Lee-Taylor, A. Robock, Multidecadal global cooling and unprecedented ozone loss following a regional nuclear conflict. *Earth's Future* **2**, 161–176 (2014).
13. J. Jägermeyr, *et al.*, A regional nuclear conflict would compromise global food security. *PNAS* **117**, 7071–7081 (2020).
14. A. Robock, *et al.*, Climatic consequences of regional nuclear conflicts. *Atmos. Chem. Phys.* **7**, 2003–2012 (2007).
15. M. Rivers, *et al.*, "Deployment of Resilient Foods Can Greatly Reduce Faminein an Abrupt Sunlight Reduction Scenario" (In Review, 2022) https:/doi.org/10.21203/rs.3.rs-1446444/v1 (August 18, 2022).
16. T. Do, K. Anderson, B. W. Brorsen, The World's wheat supply. *Oklahoma Cooperative Extension Service* (2010).
17. K. J. N. Scherrer, *et al.*, Marine wild-capture fisheries after nuclear war. *PNAS* **117**, 29748–29758 (2020).
18. A. Tzachor, C. E. Richards, L. Holt, Future foods for risk-resilient diets. *Nat Food* **2**, 326–329 (2021).
19. D. J. Winstead, M. G. Jacobson, Food resilience in a dark catastrophe: A new way of looking at tropical wild edible plants. *Ambio* **51**, 1949–1962 (2022).
20. D. C. Denkenberger, J. M. Pearce, Feeding everyone: Solving the food crisis in event of global catastrophes that kill crops or obscure the sun. *Futures* **72**, 57–68 (2015).
21. D. Denkenberger, J. Pearce, A. R. Taylor, R. Black, Food without sun: price and life-saving potential. *Foresight* **21**, 118–129 (2019).
22. J. M. Pearce, M. Khaksari, D. Denkenberger, Preliminary Automated Determination of Edibility of Alternative Foods: Non-Targeted Screening for Toxins in Red Maple Leaf Concentrate. *Plants (Basel)* **8** (2019).
23. K. A. Alvarado, A. Mill, J. M. Pearce, A. Vocaet, D. Denkenberger, Scaling of greenhouse crop production in low sunlight scenarios. *Science of The Total Environment* **707**, 136012 (2020).
24. J. B. García Martínez, J. M. Pearce, J. Throup, J. Cates, D. C. Denkenberger, Methane

Single Cell Protein: securing protein supply during global food catastrophes (2020) https:/doi.org/10.31219/osf.io/94mkg.
25. J. B. García Martínez, M. M. Brown, X. Christodoulou, K. A. Alvarado, D. C. Denkenberger, Potential of microbial electrosynthesis for contributing to food production using CO2 during global agriculture-inhibiting disasters. *Cleaner Engineering and Technology* **4** (2021).
26. J. Throup, *et al.*, Rapid repurposing of pulp and paper mills, biorefineries, and breweries for lignocellulosic sugar production in global food catastrophes. *Food and Bioproducts Processing* **131**, 22–39 (2022).
27. J. B. García Martínez, K. A. Alvarado, D. C. Denkenberger, Synthetic fat from petroleum as a resilient food for global catastrophes: Preliminary techno-economic assessment and technology roadmap. *Chemical Engineering Research and Design* **177**, 255–272 (2022).
28. C. Yarish, *et al.*, "Seaweed Aquaculture for Food Security, Income Generation and Environmental Health in Tropical Developing Countries" (World Bank Group, 2016).
29. R. P. John, G. S. Anisha, K. M. Nampoothiri, A. Pandey, Micro and macroalgal biomass: A renewable source for bioethanol. *Bioresource Technology* **102**, 186–193 (2011).
30. J. A. DeBoer, *The Marine Plant Resources and Their Aquaculture Potential in the Bahamas: A Report to the Fisheries Training and Development Project (BHA/78/001), Nassau, Bahamas* (FAO, 1981).
31. D. J. McHugh, *A Guide to the Seaweed Industry* (Food and Agriculture Organization of the United Nations, 2003).
32. F. Ferdouse, *et al.*, *The global status of seaweed production, trade and utilization* (Globlefish Research Programme, 2018).
33. N. V. Fedoroff, *et al.*, Radically Rethinking Agriculture for the 21st Century. *Science* **327**, 833–834 (2010).
34. O. G. Mouritsen, *et al.*, On the human consumption of the red seaweed dulse (Palmaria palmata (L.) Weber & Mohr). *J Appl Phycol* **25**, 1777–1791 (2013).
35. M. J. Mills, O. B. Toon, R. P. Turco, D. E. Kinnison, R. R. Garcia, Massive global ozone loss predicted following regional nuclear conflict. *Proceedings of the National Academy of Sciences* **105**, 5307–5312 (2008).
36. C. G. Bardeen, *et al.*, Extreme Ozone Loss Following Nuclear War Results in Enhanced Surface Ultraviolet Radiation. *Journal of Geophysical Research: Atmospheres* **126**, e2021JD035079 (2021).
37. L. Xu, *et al.*, The Effect of Super Volcanic Eruptions on Ozone Depletion in a Chemistry-Climate Model. *Adv. Atmos. Sci.* **36**, 823–836 (2019).
38. Y. Lehahn, K. N. Ingle, A. Golberg, Global potential of offshore and shallow waters macroalgal biorefineries to provide for food, chemicals and energy: feasibility and sustainability. *Algal Research* **17**, 150–160 (2016).
39. C. Greene, *et al.*, Transforming the Future of Marine Aquaculture: A Circular Economy Approach. *Oceanog*, 26–34 (2022).
40. H. E. Froehlich, J. C. Afflerbach, M. Frazier, B. S. Halpern, Blue Growth Potential to Mitigate Climate Change through Seaweed Offsetting. *Current Biology* **29**, 3087-3093.e3 (2019).
41. C. S. Harrison, *et al.*, A New Ocean State After Nuclear War. *AGU Advances* **3** (2022).
42. N. L. Bird, L. C.-M. Chen, J. McLachlan, Effects of Temperature, Light and Salinity on Growth in Culture of Chondrus crispus. Furcellaria lumbricalis, Gracilaria tikvahiae (Gigartinales, Rhodophyta), and Fucus serratus (Fucales, Phaeophyta). *Botanica Marina* **22** (1979).
43. B. E. Lapointe, J. H. Ryther, Some aspects of the growth and yield of Gracilaria tikvahiae in culture. *Aquaculture* **15**, 185–193 (1978).
44. I. A. Abbott, The uses of seaweed as food in Hawaii. *Econ Bot* **32**, 409–412 (1978).
45. A. H. Buschmann, *et al.*, Seaweed production: overview of the global state of exploitation,

farming and emerging research activity. *European Journal of Phycology* **52**, 391–406 (2017).
46. X. Xiao, *et al.*, Resource (Light and Nitrogen) and Density-Dependence of Seaweed Growth. *Frontiers in Marine Science* **6** (2019).
47. J. Coupe, *et al.*, Nuclear Niño response observed in simulations of nuclear war scenarios. *Commun Earth Environ* **2**, 1–11 (2021).
48. J. DeAngelo, *et al.*, Economic and biophysical limits to seaweed farming for climate change mitigation. *Nat. Plants*, 1–13 (2022).
49. C. M. Duarte, J. Wu, X. Xiao, A. Bruhn, D. Krause-Jensen, Can Seaweed Farming Play a Role in Climate Change Mitigation and Adaptation? *Front. Mar. Sci.* **4** (2017).
50. L. Xia, *et al.*, Global food insecurity and famine from reduced crop, marine fishery and livestock production due to climate disruption from nuclear war soot injection. *Nat Food*, 1–11 (2022).
51. C. A. Penniman, A. C. Mathieson, Variation in Chemical Composition of Gracilaria tikvahiae McLachlan (Gigartinales, Rhodophyta) in the Great Bay Estuary, New Hampshire. **30**, 525–534 (1987).
52. M. Notoya, “Production of Biofuel by Macroalgae with Preservation of Marine Resources and Environment” in *Seaweeds and Their Role in Globally Changing Environments*, Cellular Origin, Life in Extreme Habitats and Astrobiology., J. Seckbach, R. Einav, A. Israel, Eds. (Springer Netherlands, 2010), pp. 217–228.
53. A. Q. Hurtado, G. S. Gerung, S. Yasir, A. T. Critchley, Cultivation of tropical red seaweeds in the BIMP-EAGA region. *J Appl Phycol* **26**, 707–718 (2014).
54. M. Boyd, N. Wilson, “Island refuges for surviving nuclear winter and other abrupt sun-reducing catastrophes” (In Review, 2022) https:/doi.org/10.21203/rs.3.rs-1927222/v1 (September 1, 2022).
55. D. Soto, C. Wurmann, *Offshore Aquaculture: A Needed New Frontier for Farmed Fish at Sea* (Brill Nijhoff, 2019).
56. S. O. Olanrewaju, A. Magee, A. S. A. Kader, K. F. Tee, Simulation of offshore aquaculture system for macro algae (seaweed) oceanic farming. *Ships and Offshore Structures* **12**, 553–562 (2017).
57. I. Fung, *et al.*, Iron supply and demand in the upper ocean (vol 14, pg 281, 2000). *Global Biogeochem. Cycles* **14**, 697–700 (2000).
58. H. Kakita, H. Kamishima, Effects of Environmental Factors and Metal Ions on Growth of the Red Alga Gracilaria Chorda Holmes (Gracilariales, Rhodophyta). *J Appl Phycol* **18**, 469 (2006).
59. Y. Suzuki, K. Kuma, I. Kudo, K. Matsunaga, Iron requirement of the brown macroalgae Laminaria japonica, Undaria pinnatifida (Phaeophyta) and the crustose coralline alga Lithophyllum yessoense (Rhodophyta), and their competition in the northern Japan Sea. *Phycologia* **34**, 201–205 (1995).
60. C. Bertram, Ocean iron fertilization in the context of the Kyoto protocol and the post-Kyoto process. *Energy Policy* **38**, 1130–1139 (2010).
61. M. Bouga, E. Combet, Emergence of Seaweed and Seaweed-Containing Foods in the UK: Focus on Labeling, Iodine Content, Toxicity and Nutrition. *Foods* **4**, 240–253 (2015).
62. T. T. Zava, D. T. Zava, Assessment of Japanese iodine intake based on seaweed consumption in Japan: a literature-based analysis. *Thyroid research* **4**, 1–7 (2011).
63. E. N. Pearce, *et al.*, Effects of Chronic Iodine Excess in a Cohort of Long-Term American Workers in West Africa. *The Journal of Clinical Endocrinology & Metabolism* **87**, 5499–5502 (2002).
64. R. Mageswaran, S. Sivasubramaniam, Preliminary studies on the iodine content of some marine algae from coastal areas of Jaffna Peninsula. *J. Natn. Sci. Foundation Sri Lanka* **12**, 173 (1984).

65. J. Teas, S. Pino, A. Critchley, L. E. Braverman, Variability of Iodine Content in Common Commercially Available Edible Seaweeds. *Thyroid* **14**, 836–841 (2004).
66. J. Chen, Evaluation of radioactivity concentrations from the Fukushima nuclear accident in fish products and associated risk to fish consumers. *Radiation Protection Dosimetry* **157**, 1–5 (2013).
67. E. M. Chapman, History of the Discovery and Early Use of Radioactive Iodine. *JAMA* **250**, 2042 (1983).
68. N. Gopal, *et al.*, “Harvest Losses in Marine Fisheries” (Society of Fisheries Technologists (India), 2012) (November 9, 2022).
69. C. M. M. Gachon, T. Sime-Ngando, M. Strittmatter, A. Chambouvet, G. H. Kim, Algal diseases: spotlight on a black box. *Trends in Plant Science* **15**, 633–640 (2010).
70. A. Santiago, R. Moreira, “Chapter 5 - Drying of edible seaweeds” in *Sustainable Seaweed Technologies*, Advances in Green and Sustainable Chemistry., M. D. Torres, S. Kraan, H. Dominguez, Eds. (Elsevier, 2020), pp. 131–154.
71. S. Forbord, *et al.*, Development of Saccharina latissima (Phaeophyceae) kelp hatcheries with year-round production of zoospores and juvenile sporophytes on culture ropes for kelp aquaculture. *J Appl Phycol* **24**, 393–399 (2012).
72. S. C. James, V. Boriah, Modeling Algae Growth in an Open-Channel Raceway. *Journal of Computational Biology* **17**, 895–906 (2010).
73. C. F. D. Gurgel, S. Fredericq, J. N. Norris, Phylogeography of Gracilaria Tikvahiae (gracilariaceae, Rhodophyta): A Study of Genetic Discontinuity in a Continuously Distributed Species Based on Molecular Evidence1. *Journal of Phycology* **40**, 748–758 (2004).
74. A. Eggert, “Seaweed Responses to Temperature” in *Seaweed Biology: Novel Insights into Ecophysiology, Ecology and Utilization*, Ecological Studies., C. Wiencke, K. Bischof, Eds. (Springer, 2012), pp. 47–66.
75. J. K. Kim, C. Yarish, Development of a sustainable land-based Gracilaria cultivation system. *ALGAE* **29**, 217–225 (2014).
76. H. S. Parker, Effects of simulated current on the growth rate and nitrogen metabolism of Gracilaria tikvahiae (Rhodophyta). *Mar. Biol.* **69**, 137–145 (1982).
77. F. U. Jehn, M. Rivers, E. Ilin, allfed/Seaweed-Growth-Model: Release for Submission (2023) https:/doi.org/10.5281/ZENODO.7575050 (January 27, 2023).
78. F. U. Jehn, *et al.*, Seaweed In Nuclear Winter Data Repository (2023) https:/doi.org/10.5281/ZENODO.7553874 (January 20, 2023).
79. M. Müller, Ed., “Dynamic Time Warping” in *Information Retrieval for Music and Motion*, (Springer, 2007), pp. 69–84.
80. R. Tavenard, *et al.*, Tslearn, A Machine Learning Toolkit for Time Series Data. *Journal of Machine Learning Research* **21**, 1–6 (2020).
81. F. U. Jehn, F. J. Dingal, allfed/Seaweed-Scaleup-Model: Release for Submission (2023) https:/doi.org/10.5281/ZENODO.7575045 (January 27, 2023).
82. J. J. Milledge, B. Smith, P. W. Dyer, P. Harvey, Macroalgae-Derived Biofuel: A Review of Methods of Energy Extraction from Seaweed Biomass. *Energies* **7**, 7194–7222 (2014).
83. P. D. Lewis, Responses of domestic fowl to excess iodine: a review. *Br J Nutr* **91**, 29–39 (2004).
84. H. R. Hansen, B. L. Hector, J. Feldmann, A qualitative and quantitative evaluation of the seaweed diet of North Ronaldsay sheep. *Animal Feed Science and Technology* **105**, 21–28 (2003).
85. Automobile Manufacturers Association, *Freedom’s Arsenal: The Story of the Automotive Council for War Production* (Automobile Manufacturers Association, 1950).
86. D. J. Steenbergen, C. Marlessy, E. Holle, Effects of rapid livelihood transitions: Examining local co-developed change following a seaweed farming boom. *Marine Policy* **82**, 216–223

(2017).
87. Statista, “Global textile fiber production by type 2021” (January 26, 2023).
88. P. Mineault, K. Nozawa, The Good Research Code Handbook (2021) https:/doi.org/10.5281/ZENODO.5796872 (July 6, 2022).

Supporting Information for “Seaweed as a resilient food solution after nuclear war”

Large Marine Ecosystem Growth Rates

The growth rates of seaweed were also calculated for all 66 large marine ecosystems (LMEs). The following are those referred to in the main manuscript. All others can be found in the repository of this paper (1).

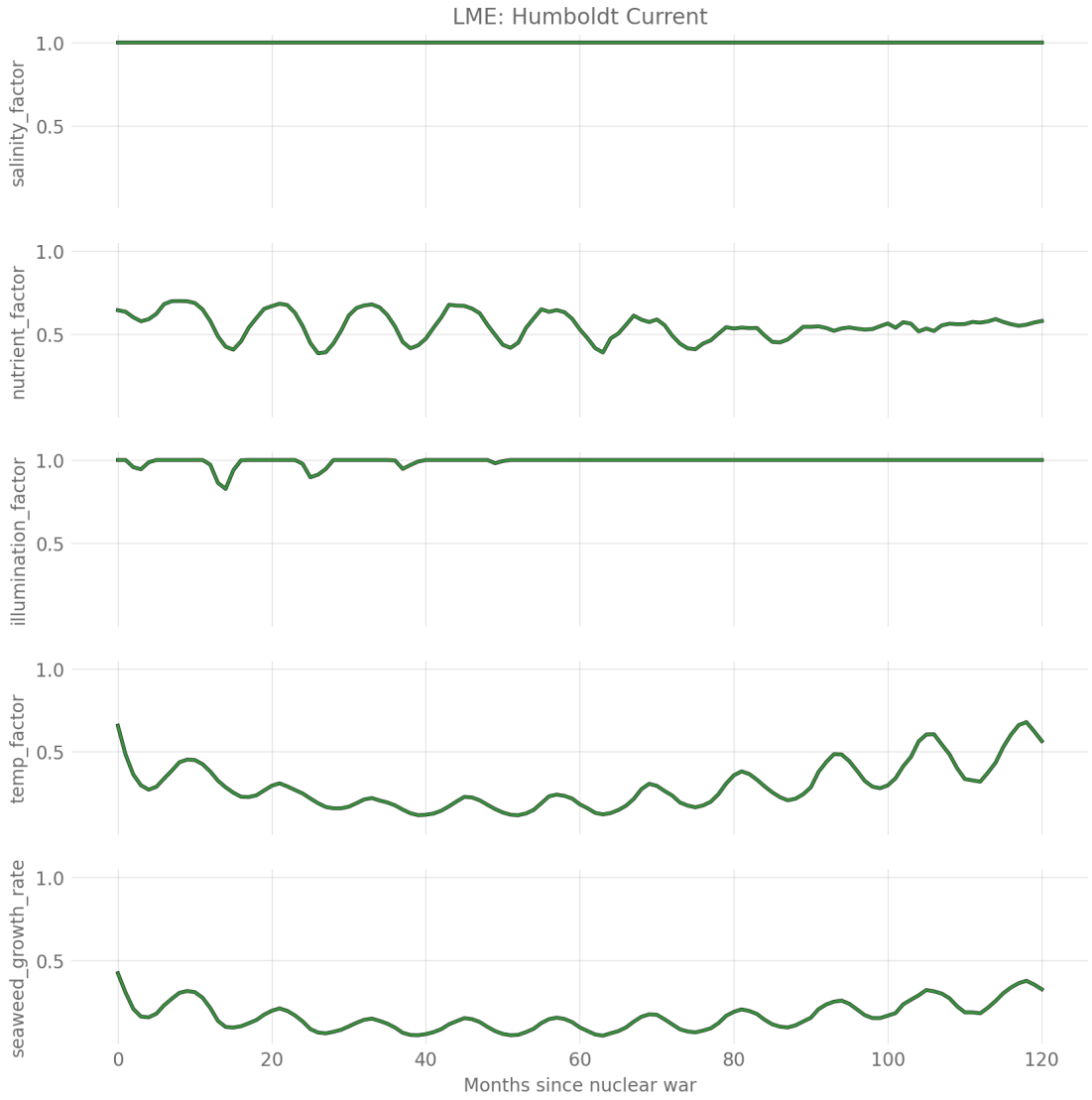


Figure S1: Time series of the growth factors (salinity, nutrients, illumination, temperature) and the overall growth rate (which is the product of the four factors) for the Humboldt Current (150 Tg).

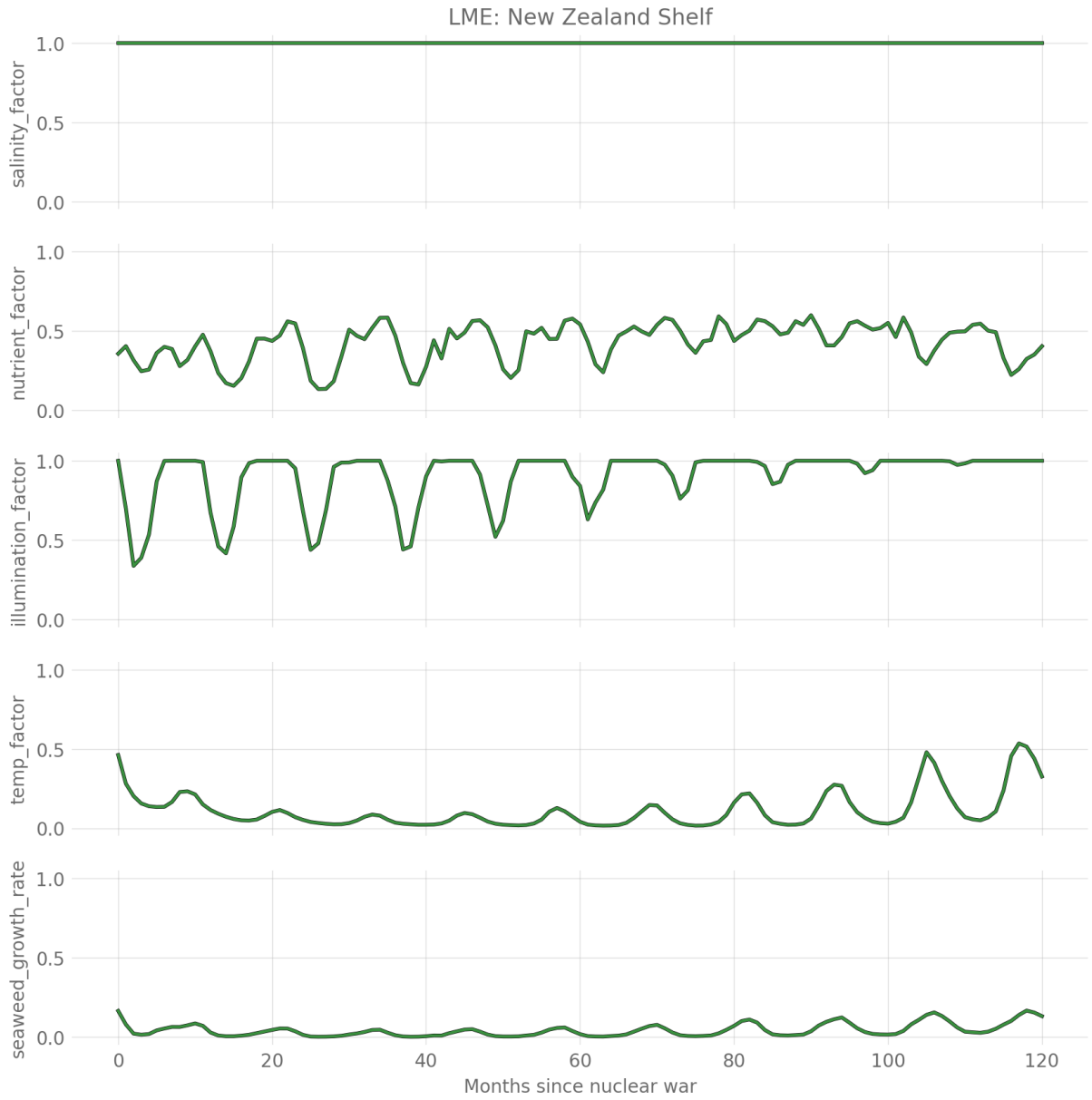


Figure S2: Time series of the growth factors (salinity, nutrients, illumination, temperature) and the overall growth rate (which is the product of the four factors) for the New Zealand Shelf (150 Tg).

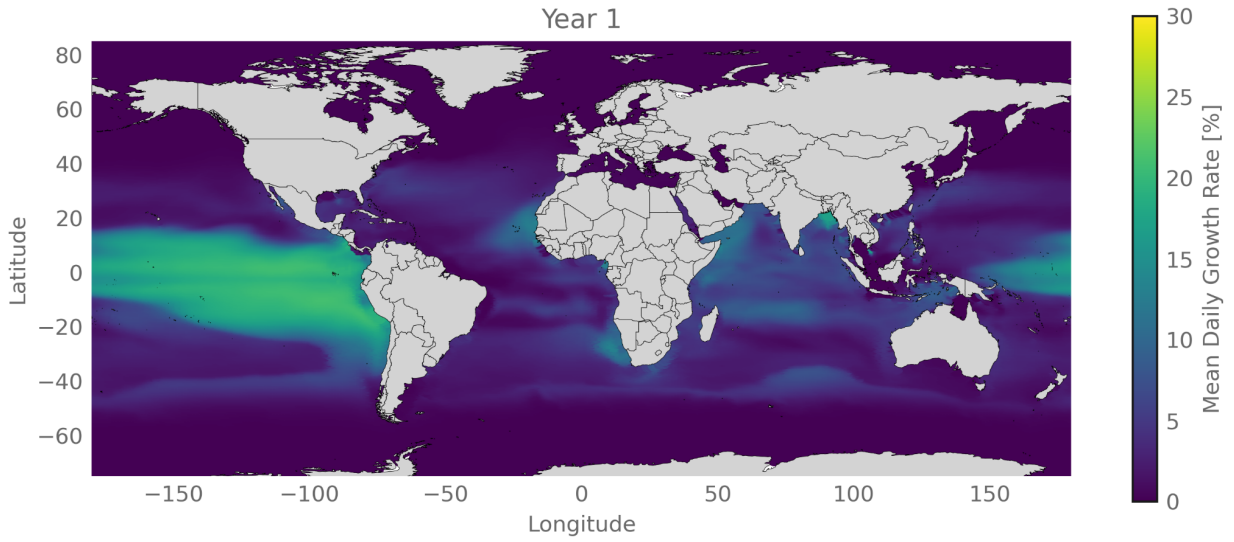


Figure S3: Global distribution of mean daily seaweed growth rates in percent per day for year 1 after the nuclear war (150 Tg).

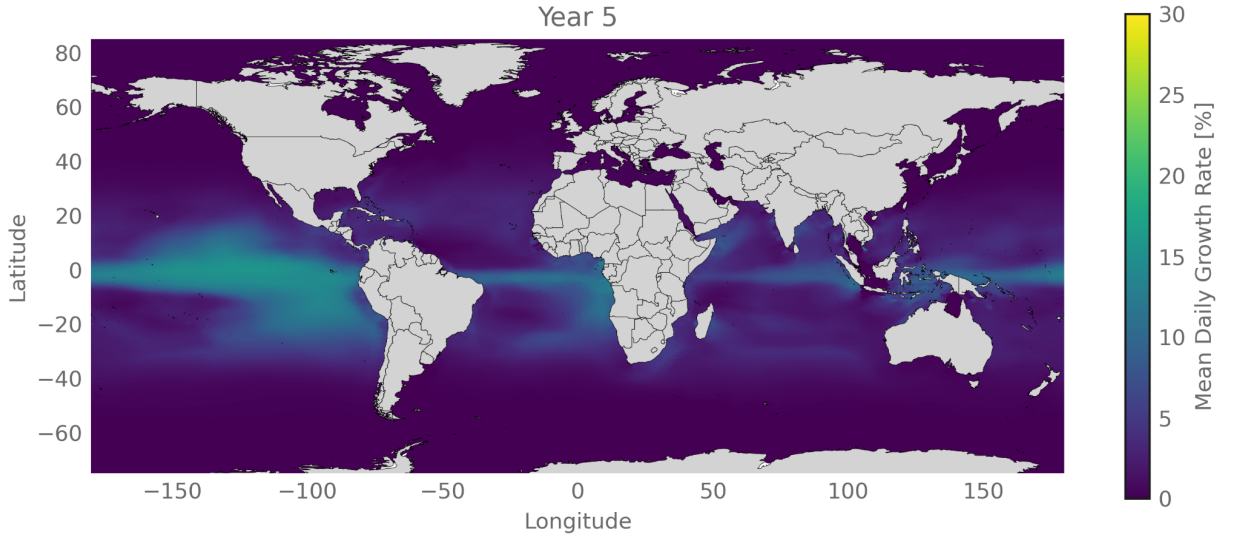


Figure S4: Global distribution of mean daily seaweed growth rates in percent for per day year 5 after the nuclear war (150 Tg).

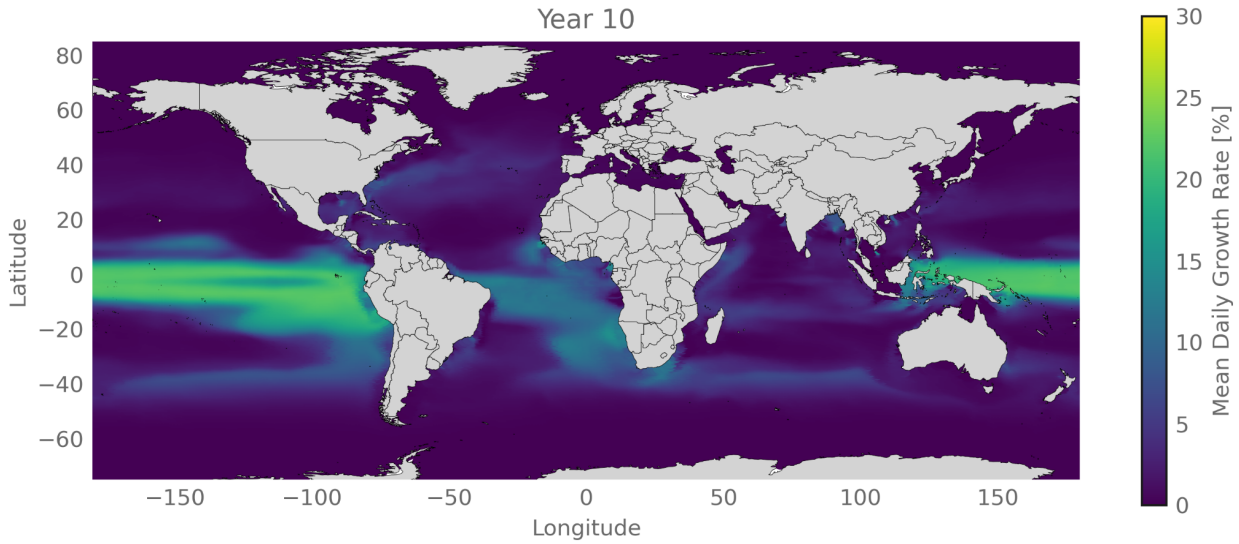


Figure S5: Global distribution of mean daily seaweed growth rates in percent per day for year 10 after the nuclear war (150 Tg).

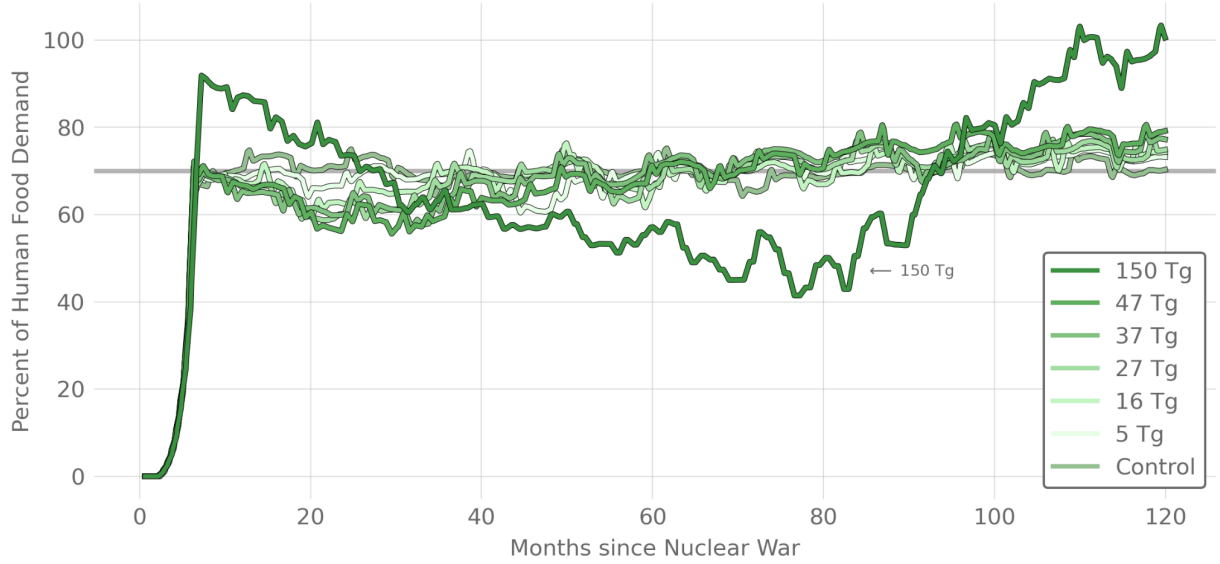


Figure S6: Food satisfaction of the global population by seaweed for the fastest growing cluster in all nuclear war scenarios and the control run.



Figure S7: Examples of low tech seaweed farming (Copyright: Michael Y. Roleda).

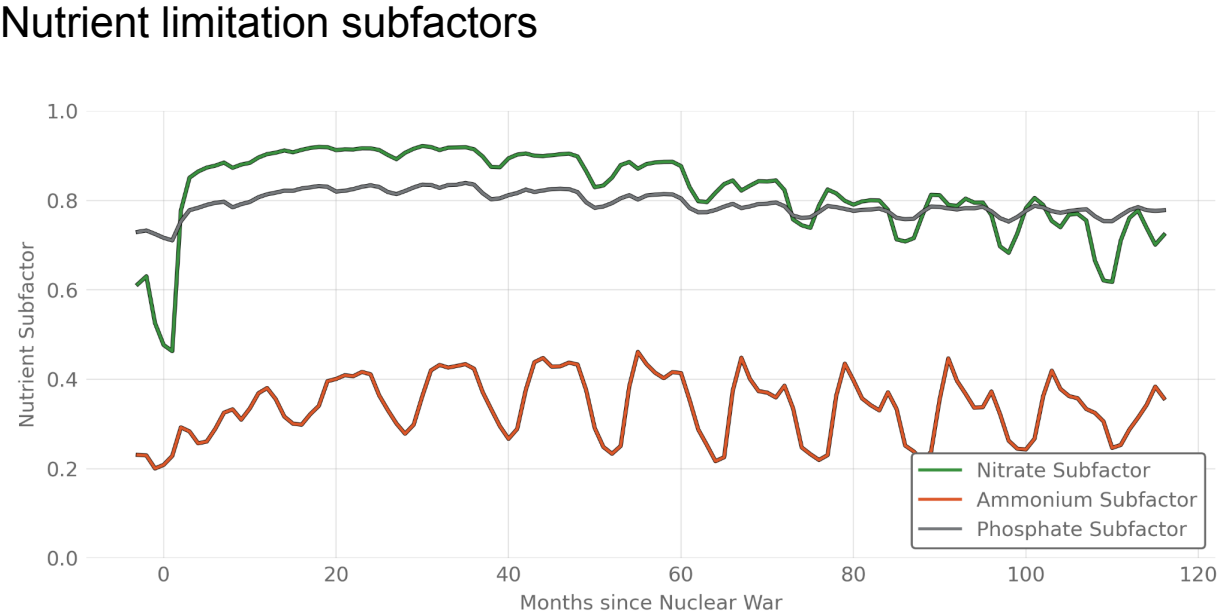


Figure S8: Global median of the three nutrient subfactors (150 Tg).

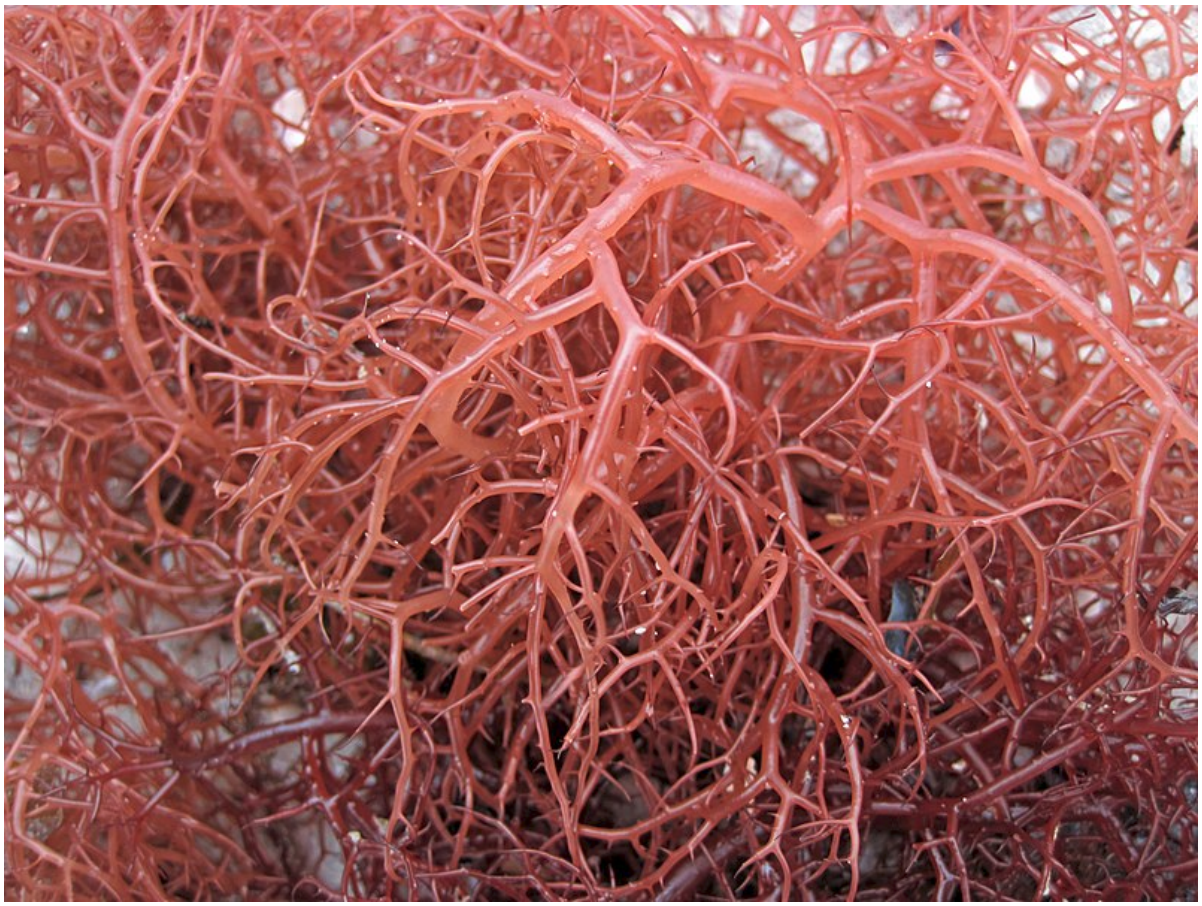


Figure S9: Morphology of Gracilaria tikvahiae (Photo by James St. John, CC BY)

Growth Limitation Functions

The following equations are the ones used to calculate the growth factors in the seaweed growth model. They are based on Scott and Boriah (2010) (2), who used growth data from experiments with *Gracilaria tikvahiae* and built an empirical model that could reproduce the growth data. All factors can experience values between 0 and 1, where 0 means no growth and 1 is optimal growth.

Light

Experimental data (3, 4) shows that *Gracilaria tikvahiae* becomes light saturated at 21.9 W per m² and experiences an inhibition of growth starting at values of 109.5 W per m². Between 0 and 21.9 W per m² we see a steep increase in growth, while we see a slow decline in growth if the seaweed becomes oversaturated above 109.5 W per m². The empirical formula to reproduce the illumination (I) pattern see in the data is:

$$f(I) = \frac{I}{21.9} exp(1 - \frac{I}{21.9}) \quad for\ I > 21.9\ \frac{W}{m^2}$$

$$f(I) = 1 \quad for\ 21.9 \leq I \leq 109.5 \frac{W}{m^2}$$

$$f(I) = \frac{109.5}{I} \quad for\ I > 109.5\ \frac{W}{m^2}$$

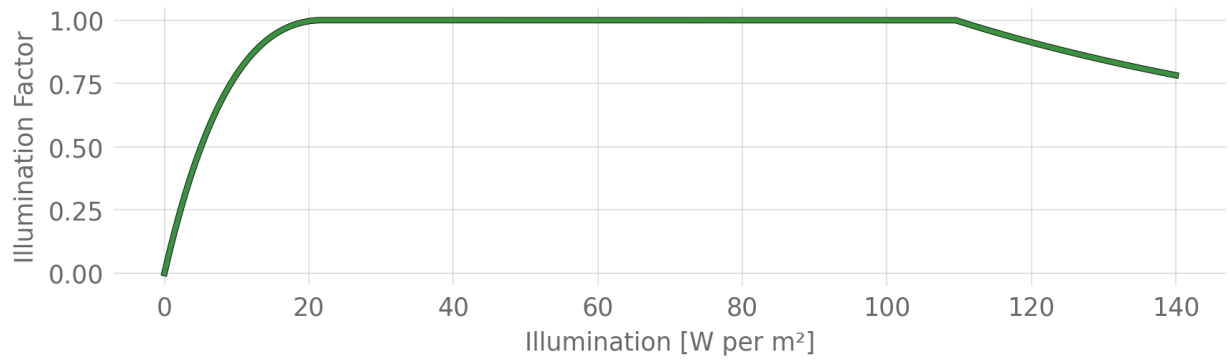


Figure S10: Gracilaria tikvahiae light-limitation function.

Temperature

Growth is reduced below 24°C and above 30°C and mostly suppressed below 7°C and above 37°C, with optimum temperatures (T) between 24 and 30°C. This is based on data by Hansiak (1987) (4). The data show a slow logistic increase between 0°C, before reaching the optimum at 24°C. A faster decline happens above 30°C when it gets too hot for the seaweed. The empirical formula to reproduce this pattern is:

$$g(T) = exp(-0.017(24 - T)^2) \quad for\ T > 24°C$$

$$g(T) = 1 \quad for\ 24 \leq T \leq 30°C$$

$$g(T) = exp(-0.064(T - 30)^2) \quad for\ T > 30°C$$

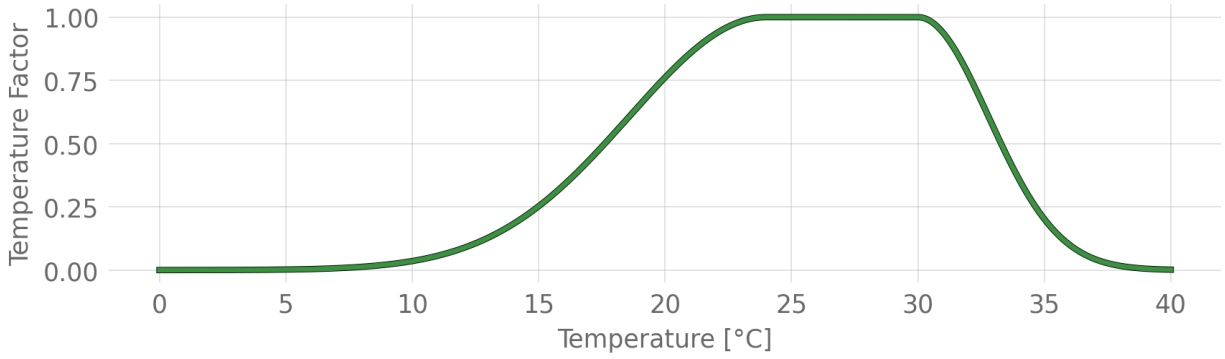


Figure S11: Gracilaria tikvahiae temperature-limitation function.

Nutrients

For nutrients no reliable data is available for *Gracilaria tikvahiae*. Therefore, data for *Gracilaria foliifera* are used (5, 6). DeBoer and D'Elia (5, 6) propose half-saturation constants (7) of 0.4 µmol/L for Nitrate (N), 0.3 µmol/L for Ammonium (A) and 0.1 µmol/L for Phosphate (P). The resulting equations are:

$$h(N) = \frac{N}{0.4 + N}$$

$$h(A) = \frac{A}{0.3 + A}$$

$$h(P) = \frac{P}{0.1 + P}$$

The nutrient factor is the minimum of the three nutrient limitation factors following Liebig's law of the minimum (8).

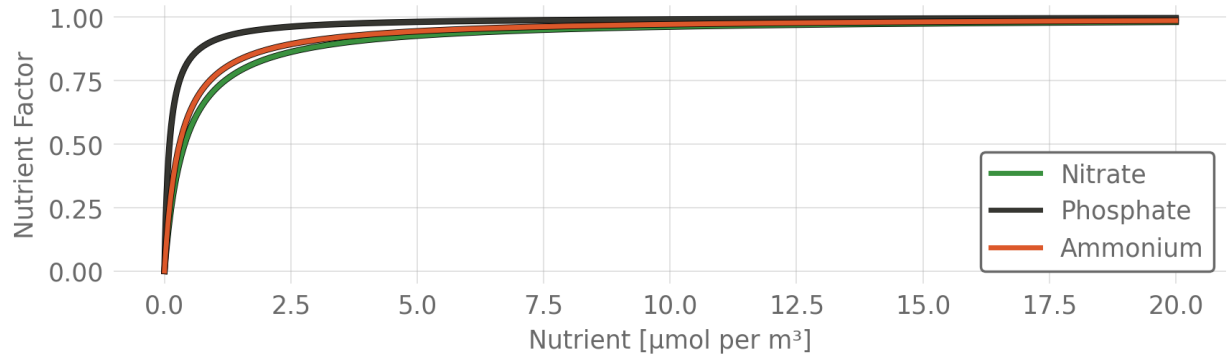


Figure S12: Gracilaria tikvahiae nutrient-limitation function.

Salinity

Growth of *Gracilaria tikvahiae* is optimal for a salinity (S) between 24 and 36 ppt (4). Higher and lower concentrations hinder the growth, but growth was still possible above 0 ppt and below 44 ppt. The empirical formula to reproduce this pattern is:

$$i(S) = exp(-0.007(24 - S)^2) \quad for\ S < 24\ ppt$$

$$i(S) = 1 \quad for\ 24 \leq S \leq 36\ ppt$$

$$i(S) = exp(-0.063(S - 36)^2) \quad for\ S > 36\ ppt$$

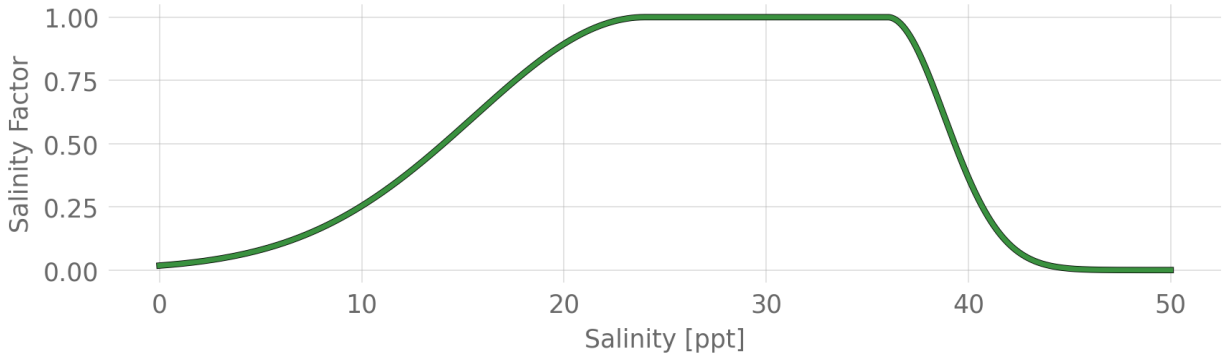


Figure S13: Gracilaria tikvahiae salinity-limitation function.

Self-Shading

The growth of *Gracilaria tikvahiae* declines above a density (D) of 0.4 kg per m² due to self-shading of the seaweed (9). The self-shading is used in the scale-up model. The empirical formula to reproduce the growth pattern is:

$$j(D) = 1 \qquad for\ D < 0.4\ \frac{kg}{m^2}$$

$$j(D) = exp(-0.513(D - 0.4)) \qquad for\ D \geq 0.4\ \frac{kg}{m^2}$$

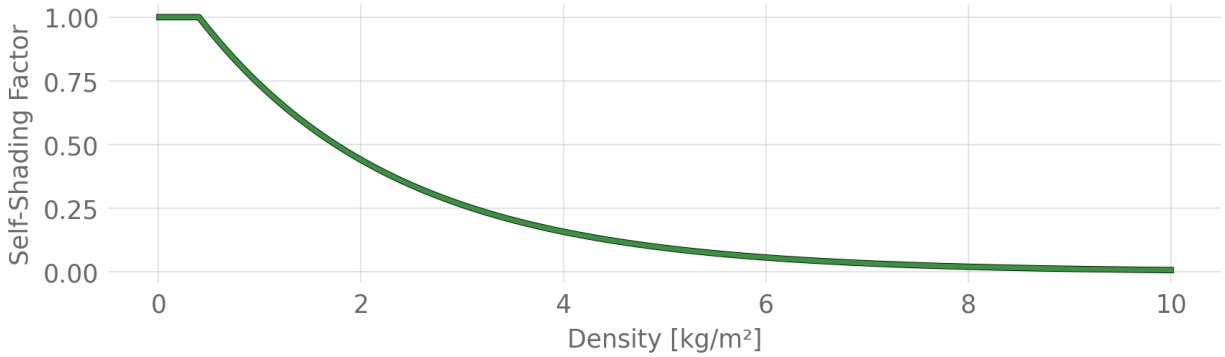


Figure S14: Gracilaria tikvahiae self-shading-limitation function.

Elbow method

To determine the best number of clusters in an unsupervised clustering method the so-called elbow method is often used. It visualizes the trade-off between trying to minimize the number of clusters with having the most accurate model of the data. The elbow of the plot identifies the best numbers of clusters for this trade-off (10). In the case of this study, a good trade-off can be found at three clusters (Figure S7).

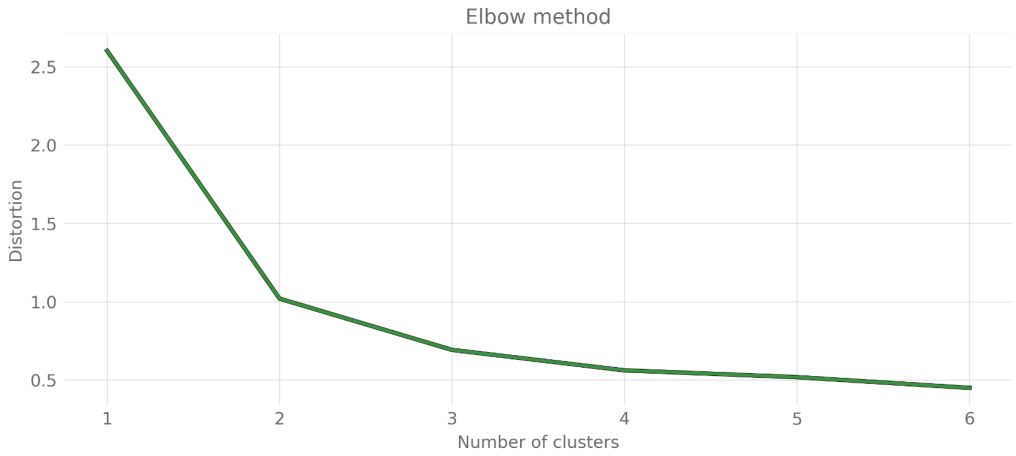


Figure S15: Distortion (sum of squared distances from each point to its assigned center) for 1 to 6 clusters (150 Tg).

Seaweed farm building scale-up

Logistic growth fit for the seaweed farm building scale up.

$$k(day) = production / (1 + exp(- k\,(day - midpoint))) + offset$$

where:

$$production = maximum\ value\ of\ production$$

$$k = the\ logistic\ growth\ rate$$

$$day = the\ current\ day$$

$$midpoint = the\ sigmoid's\ midpoint$$

$$offset = offset\ to\ 0$$

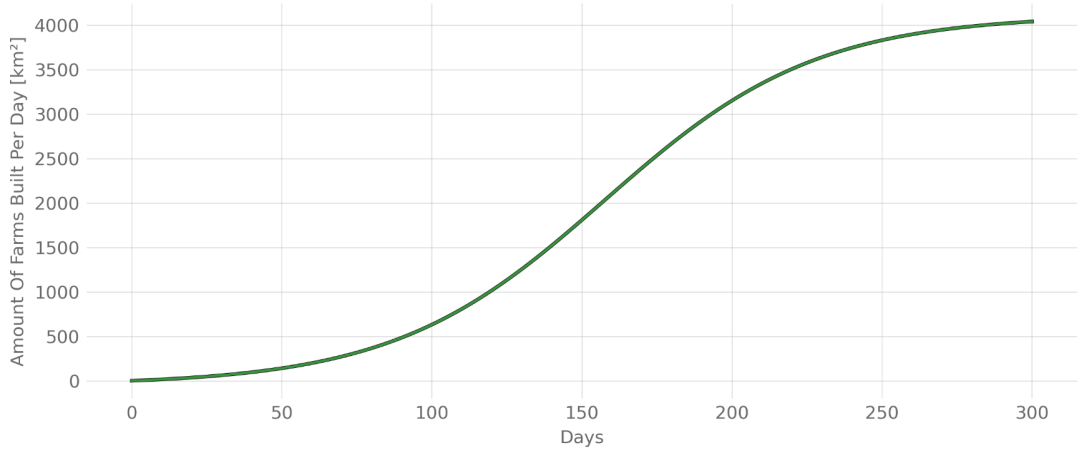


Figure S16 Logistic growth model of the amount of seaweed farms that can be built each day

References

1. F. U. Jehn, F. J. Dingal, allfed/Seaweed-Scaleup-Model: Release for Submission (2023) https:/doi.org/10.5281/ZENODO.7575045 (January 27, 2023).
2. S. C. James, V. Boriah, Modeling Algae Growth in an Open-Channel Raceway. *Journal of Computational Biology* **17**, 895–906 (2010).
3. B. E. Lapointe, M. D. Hansiak, Productivity and nutrition of marine biomass systems in Florida. *Energy from Biomass and Waste* **9** (1985).
4. M. D. Hansiak, “Cultivation of Gracilaria and other macroalgae in Florida for energy production” in *Seaweed Cultivation for Renewable Resources*, Developments in aquaculture and fisheries science., K. T. Bird, P. H. Benson, Eds. (Elsevier, 1987).
5. J. A. DeBoer, H. J. Guigli, T. L. Israel, C. F. D’Elia, Nutritional Studies of Two Red Algae. I. Growt Rate as a Function of Nitrogen Source and Concentration1. *Journal of Phycology* **14**, 261–266 (1978).
6. C. F. D’Elia, J. A. DeBoer, Nutritional Studies of Two Red Algae. Ii. Kinetics of Ammonium and Nitrate Uptake1, 2. *Journal of Phycology* **14**, 266–272 (1978).
7. C. Mulder, A. J. Hendriks, Half-saturation constants in functional responses. *Global Ecology and Conservation* **2**, 161–169 (2014).
8. R. r. van der Ploeg, W. Böhm, M. b. Kirkham, On the Origin of the Theory of Mineral Nutrition of Plants and the Law of the Minimum. *Soil Science Society of America Journal* **63**, 1055–1062 (1999).
9. B. E. Lapointe, J. H. Ryther, Some aspects of the growth and yield of Gracilaria tikvahiae in culture. *Aquaculture* **15**, 185–193 (1978).
10. R. L. Thorndike, Who belongs in the family? *Psychometrika* **18**, 267–276 (1953).